

Electronic Supporting Information

Carbazole appended *trans*-dicationic pyridinium porphyrin finds supremacy in DNA binding/photocleavage over non-carbazolyl analogue

Athulya Das,^a Thasnim P Mohammed,^a Rajesh Kumar,^a Sarmistha Bhunia,^b Muniyandi Sankaralingam^{*a}

^aBioinspired & Biomimetic Inorganic Chemistry Lab, Department of Chemistry, National Institute of Technology Calicut, Kozhikode-673601, Kerala, India.

^bSchool of Chemical Sciences, Indian Association for the Cultivation of Science, Kolkata 700032, India

*Corresponding author email: msankaralingam@nitc.ac.in; sankarjan06@gmail.com

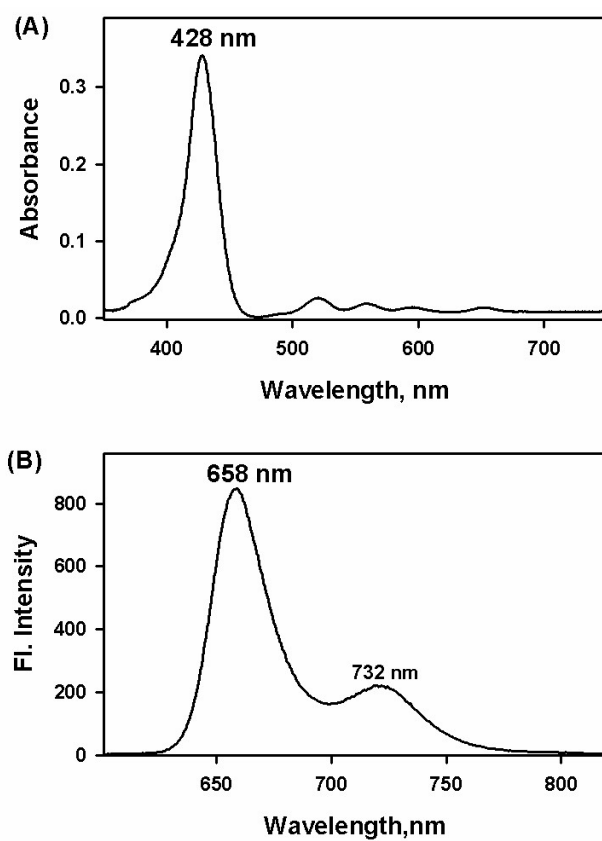


Fig. S1. (A) UV-visible absorption and (B) Fluorescence emission spectra of **1** recorded in CHCl_3 at 298 K.

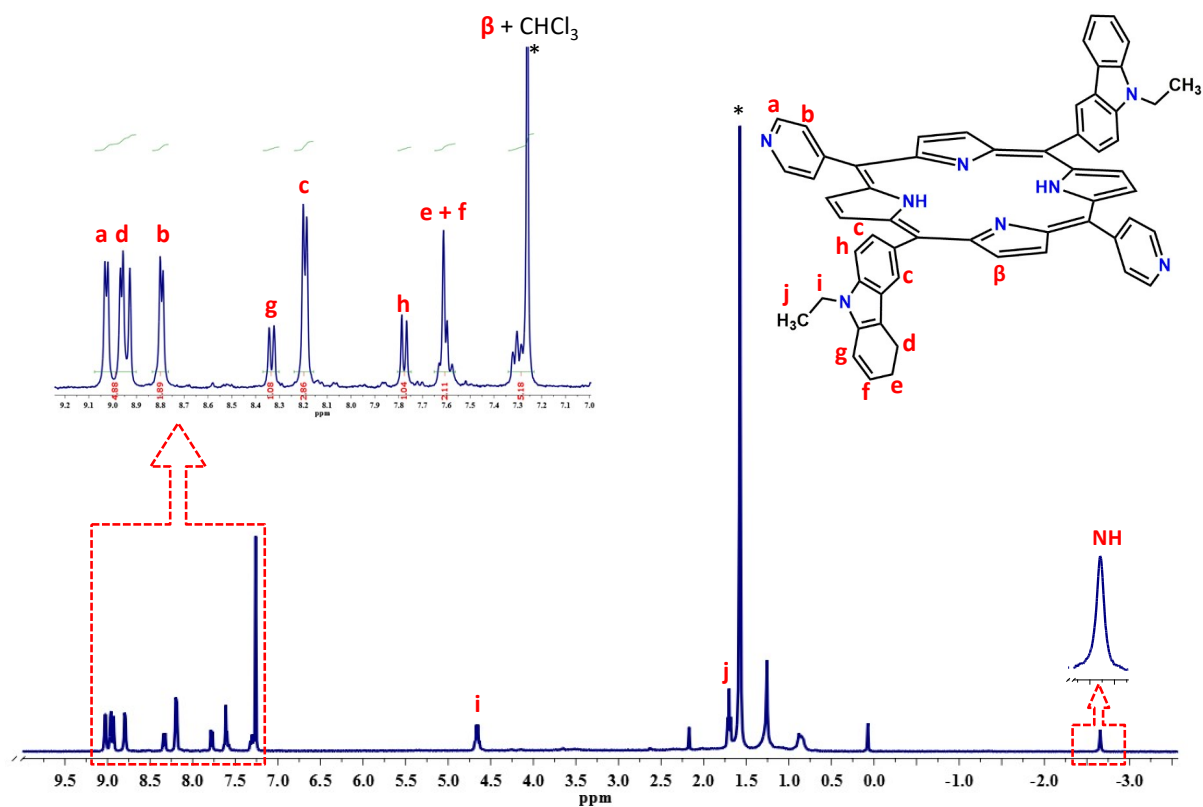


Fig. S2. ^1H NMR spectrum of **1** recorded in CDCl_3 . Marked peak with an asterisk (*) at 1.56 and 7.26 ppm indicates residual CDCl_3 and water respectively.

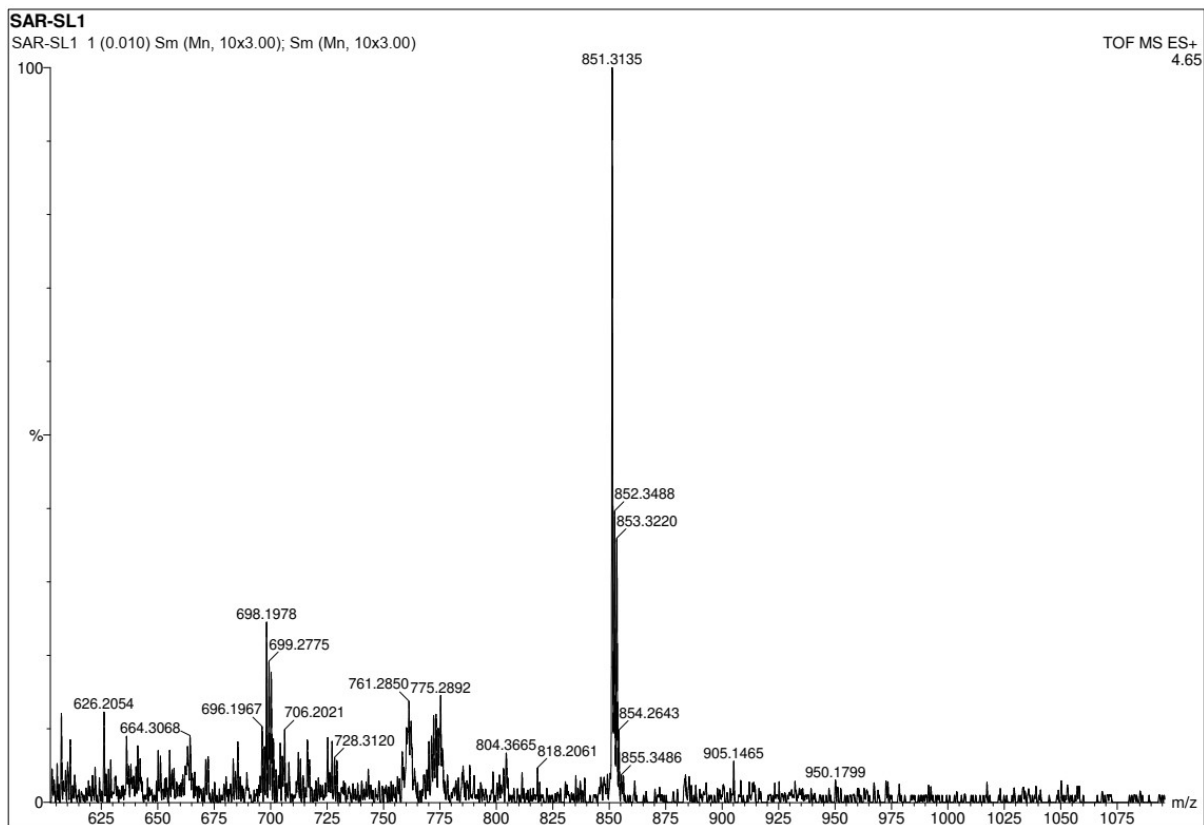


Fig. S3. Mass spectrum of **1** recorded in CHCl_3 .

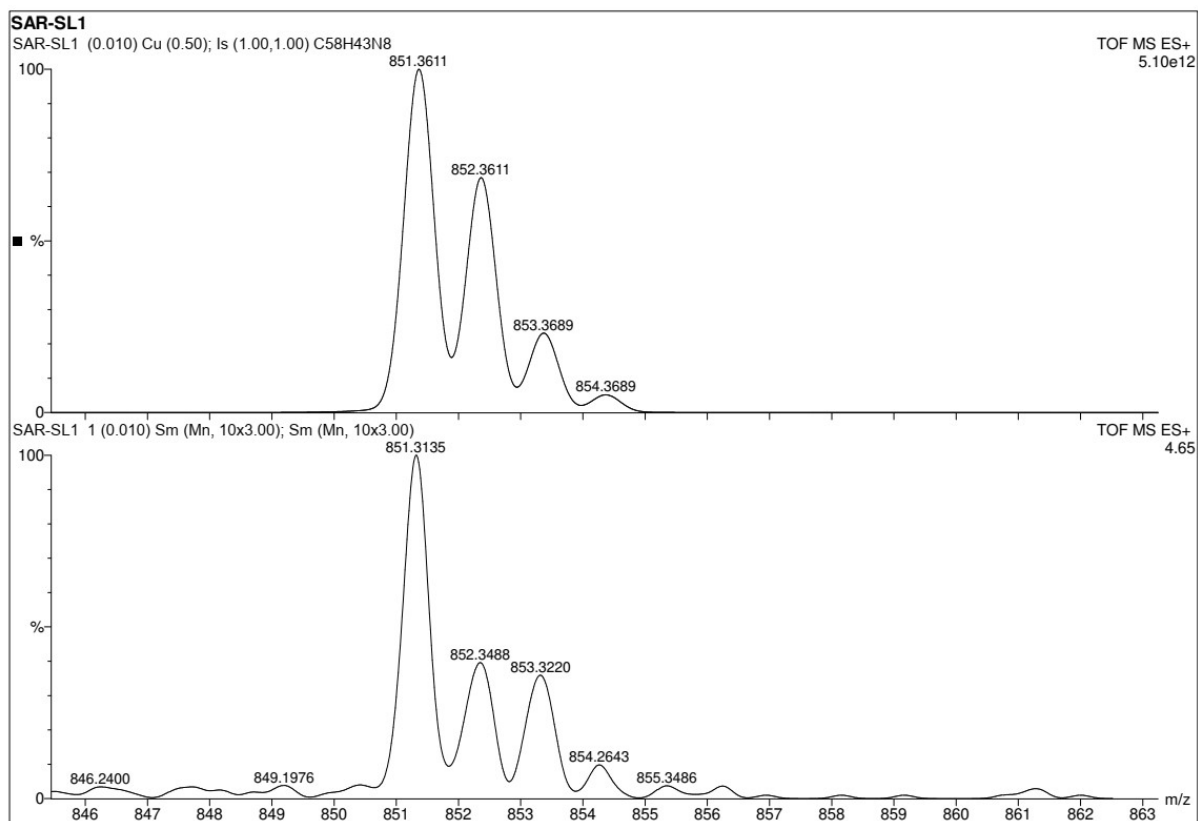


Fig. S4. Experimental (top) and theoretical (bottom) isotopic distribution of **1** was recorded in CHCl_3 .

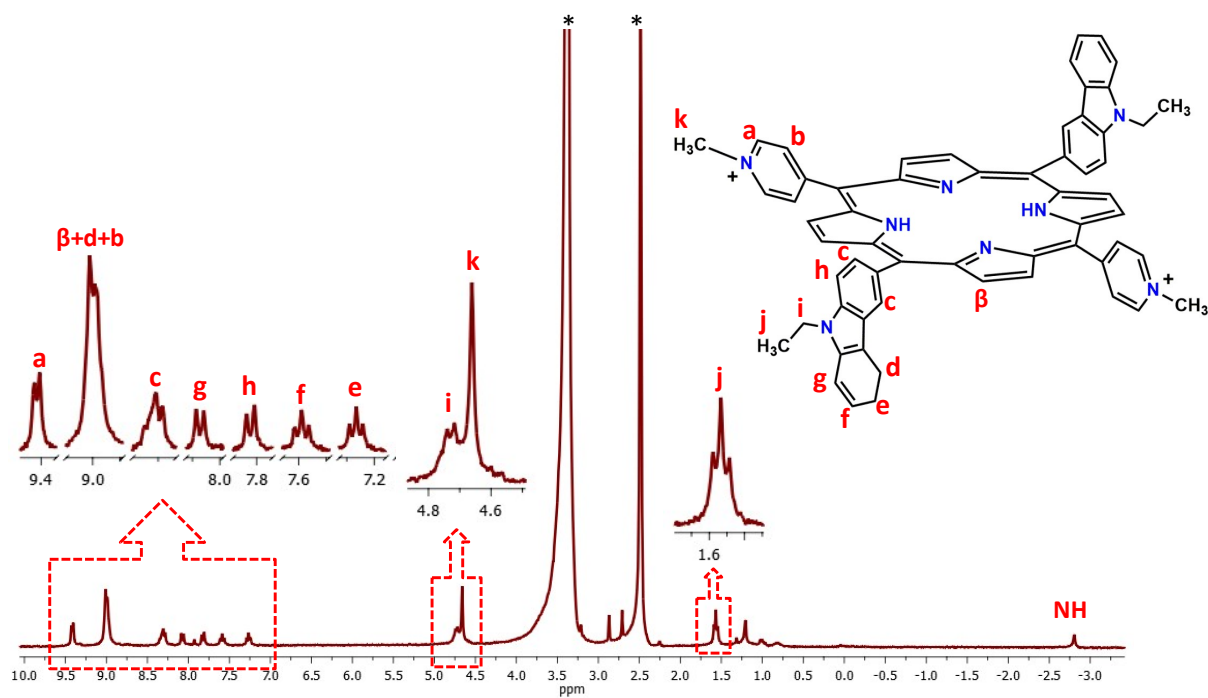


Fig. S5. ^1H NMR spectrum of **2** recorded in $\text{DMSO-}d_6$. Marked peak with an asterisk (*) at 2.5 and 3.5 ppm indicates residual DMSO and water, respectively.

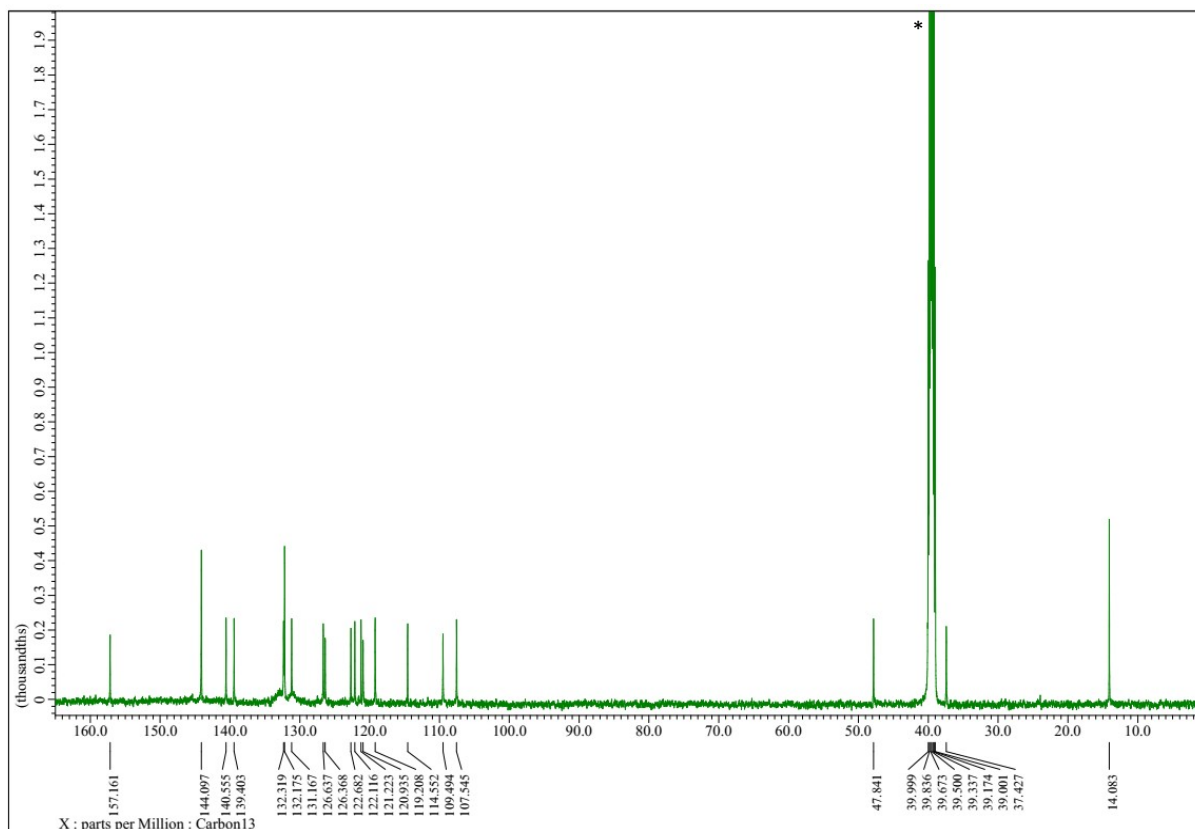


Fig. S6. ^{13}C NMR spectrum of **2** recorded in $\text{DMSO-}d_6$. Marked peak with an asterisk (*) at 39-39.9 ppm indicates residual DMSO.

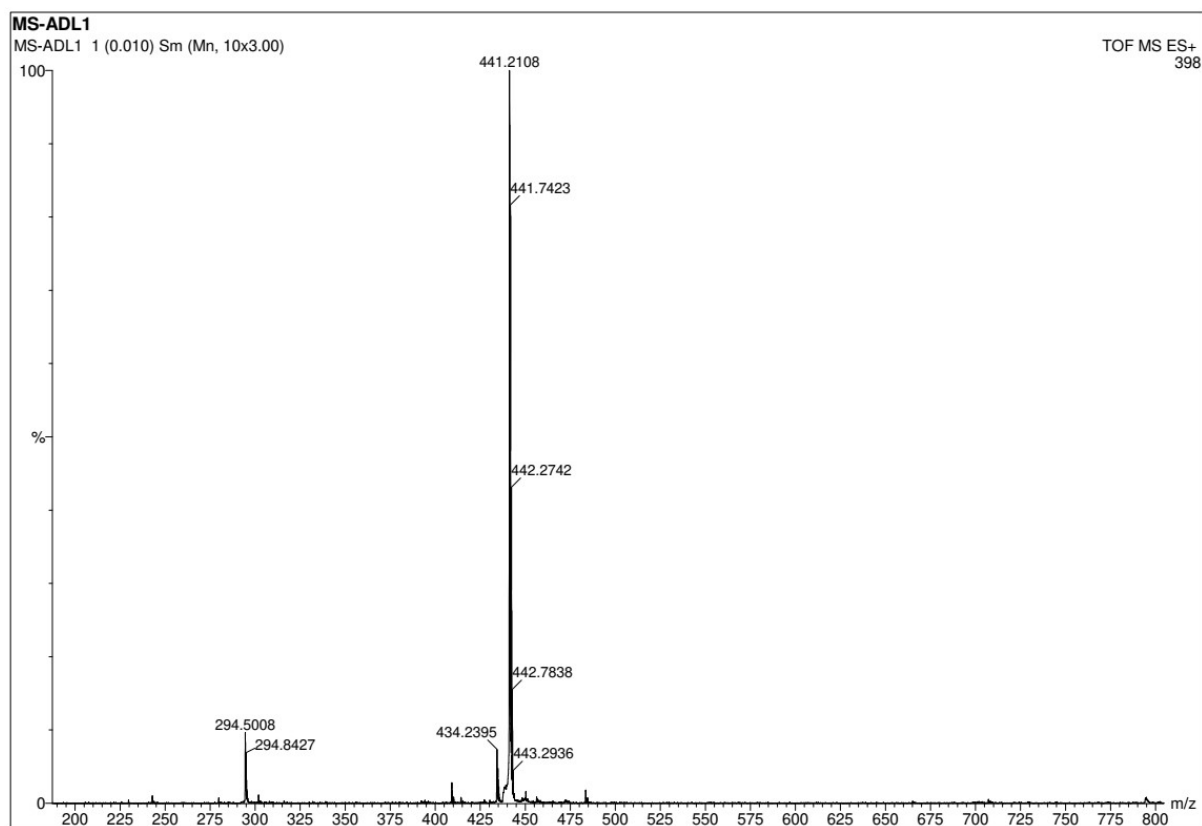


Fig. S7. Mass spectrum of **2** recorded in CH_3OH .

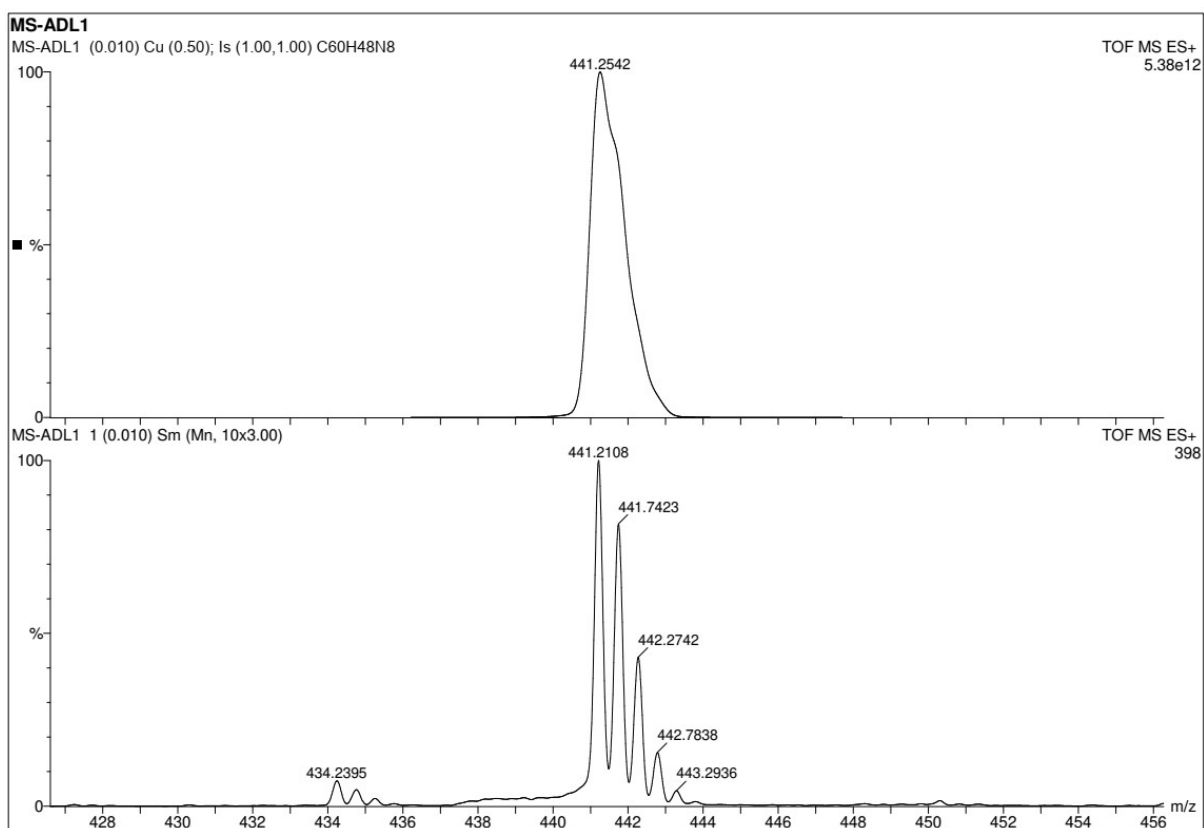


Fig. S8. Theoretical (top) experimental (bottom) isotopic distribution of **2** recorded in CH_3OH .

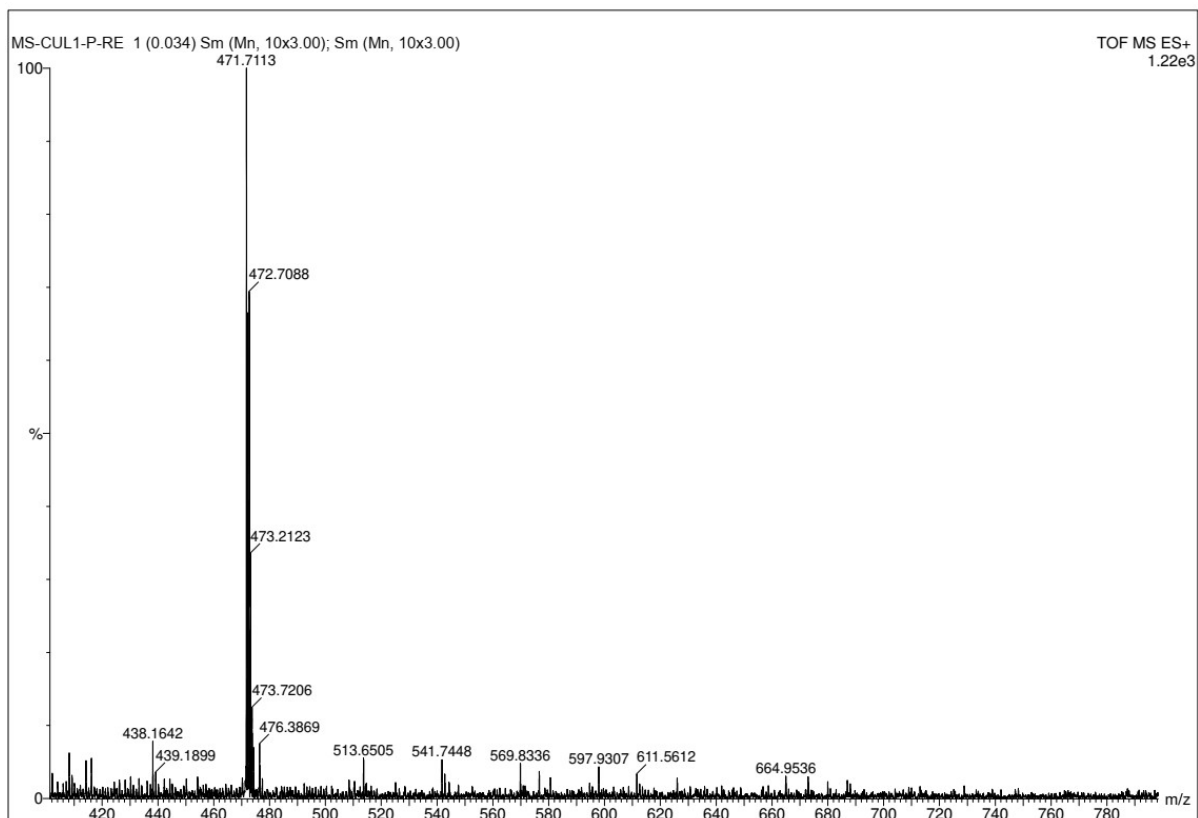


Fig. S9. Mass spectrum of **3** recorded in CH_3OH .

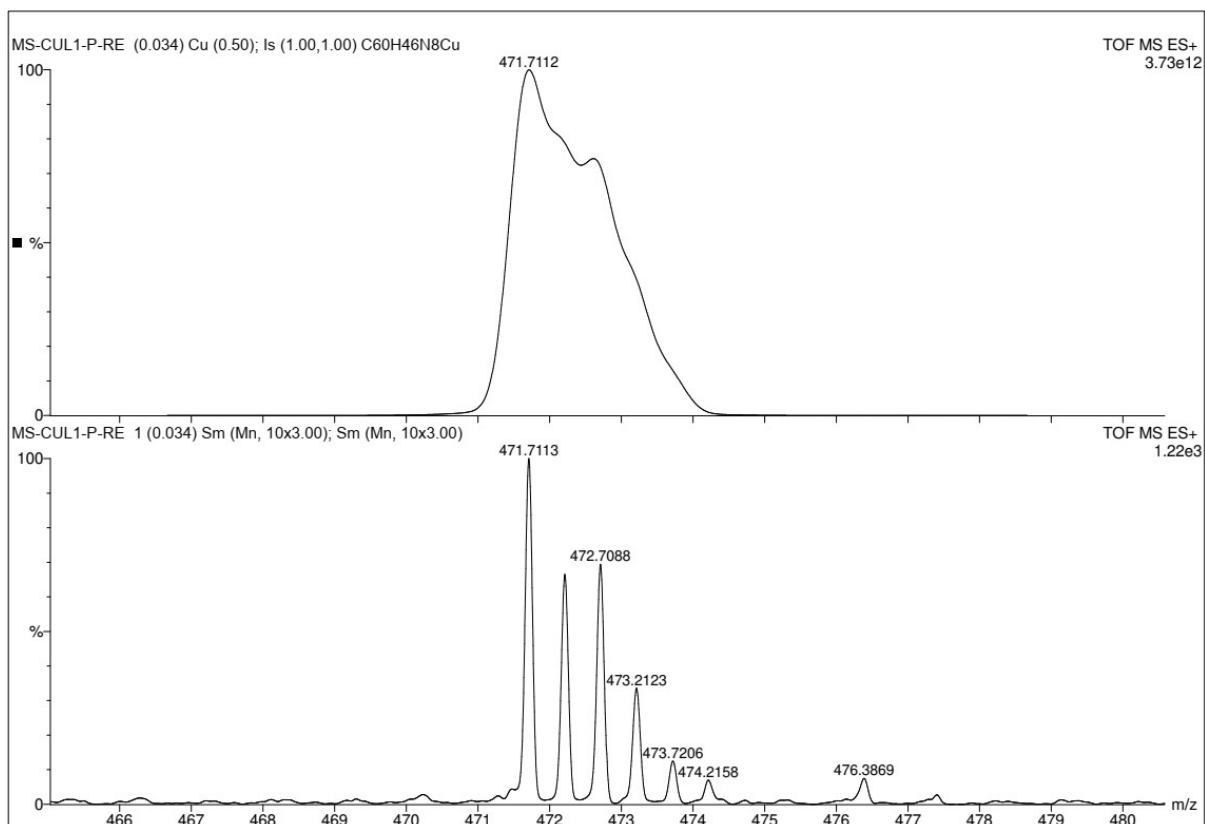


Fig. S10. Theoretical (top) experimental (bottom) isotopic distribution of **3** recorded in CH_3OH .

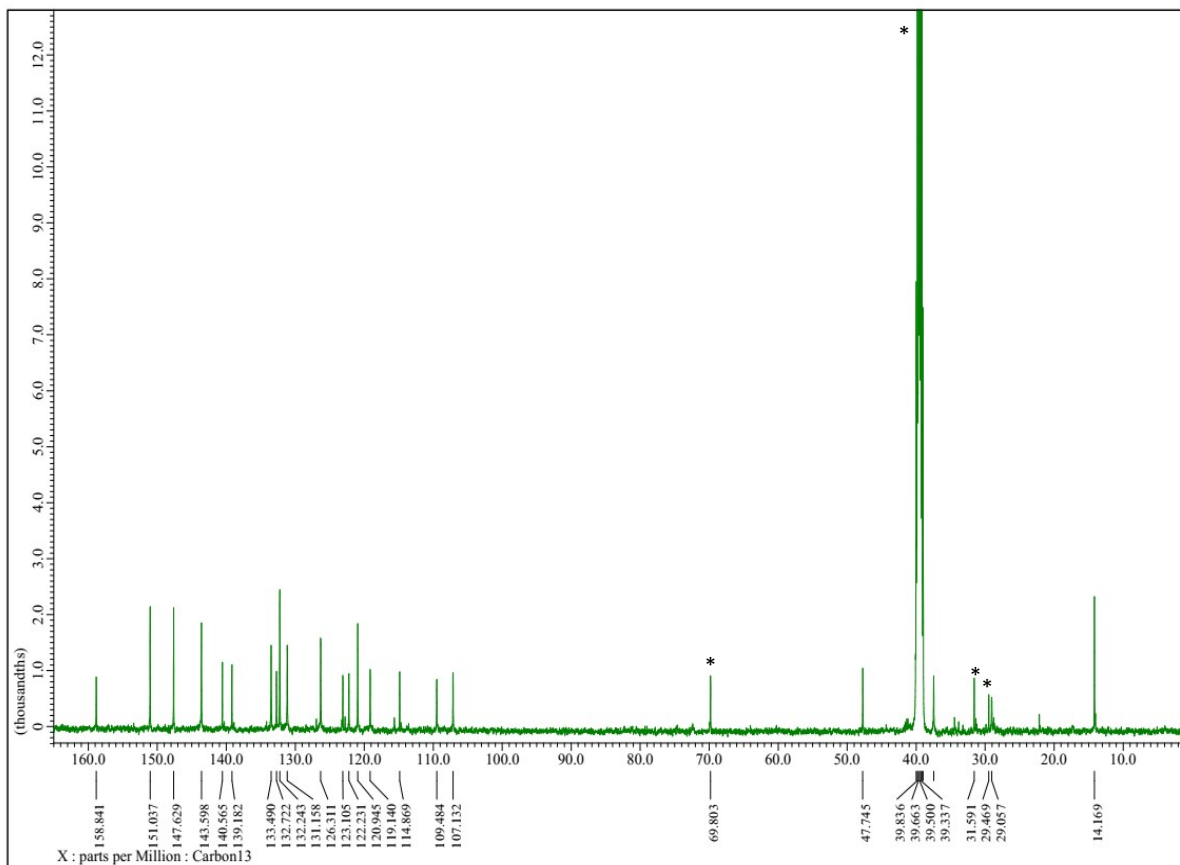


Fig. S11. ^{13}H NMR spectrum of **4** recorded in $\text{DMSO-}d_6$. Marked peak with an asterisk (*) at 39.1-39.8 ppm indicates residual DMSO, 29-31.5 ppm indicates hexane, and 69.8 ppm indicates chloroform.

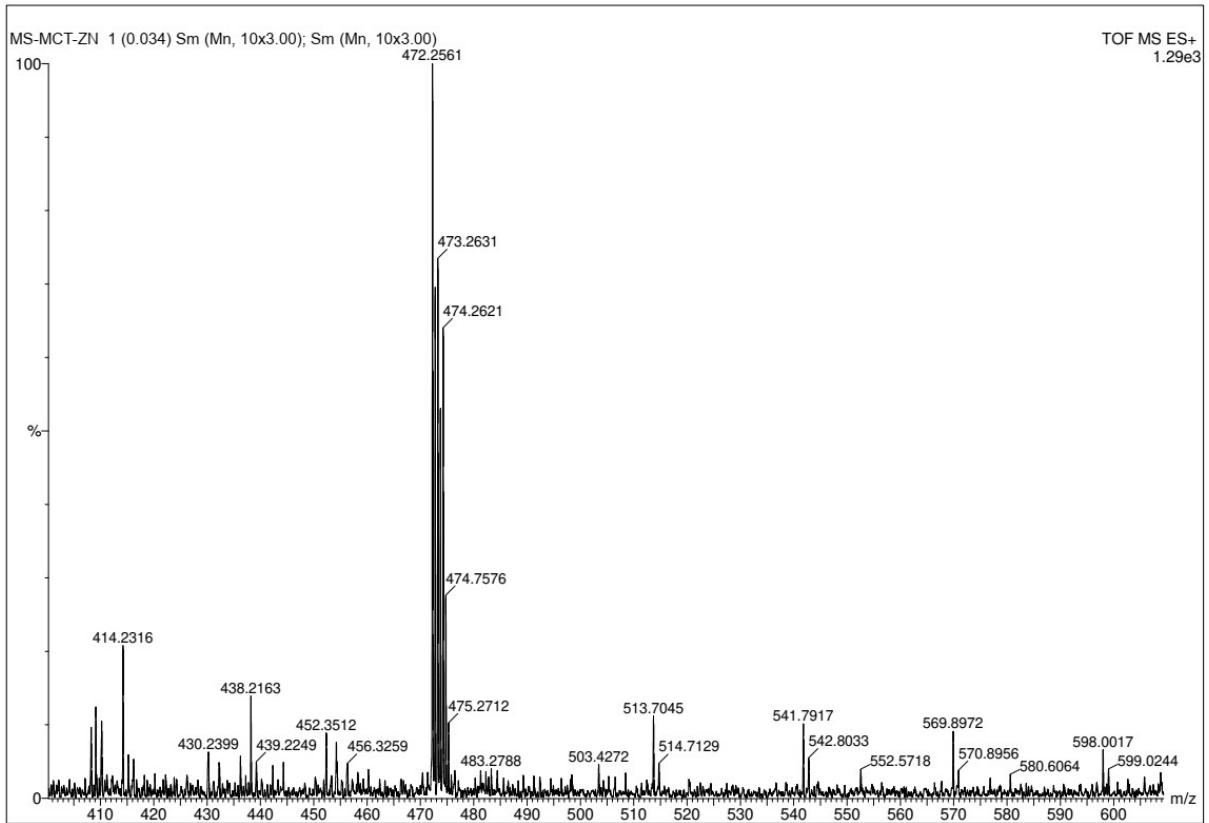


Fig. S12. Mass spectrum of **4** recorded in CH₃OH.

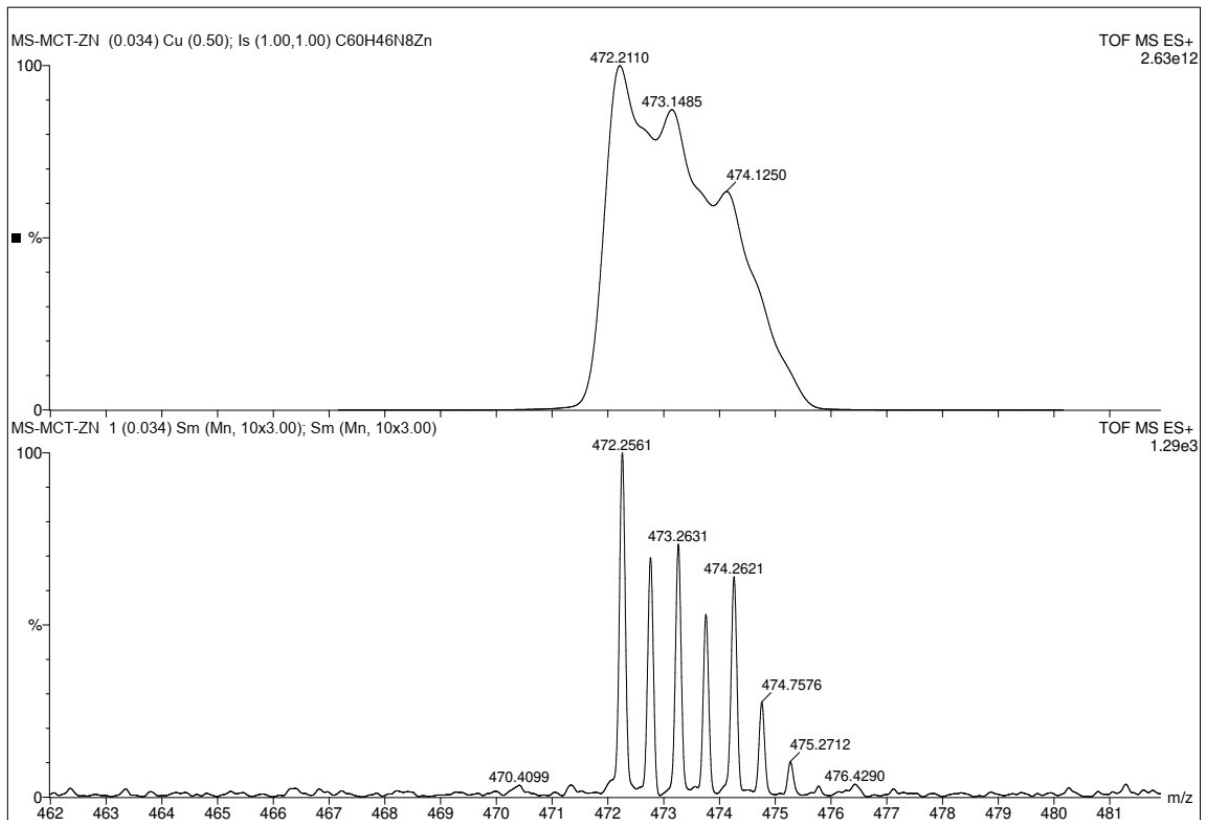


Fig. S13. Theoretical (top) experimental (bottom) isotopic distribution of **4** recorded in CH₃OH.

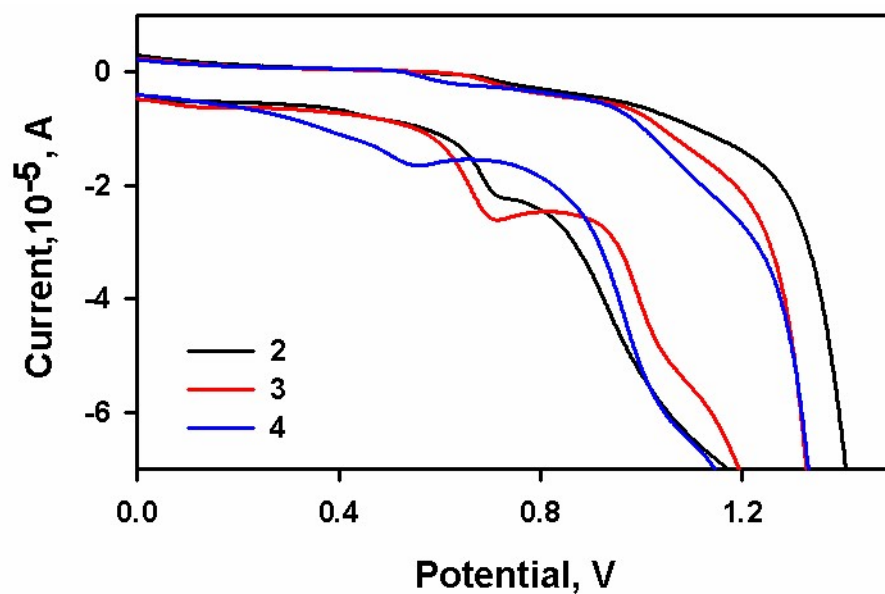


Fig. S14. Cyclic voltammograms (oxidation) of **2**, **3** and **4** in DMF containing 0.1 M tetrabutylammonium hexafluorophosphate as the supporting electrolyte with a scan rate of 0.1 V/s.

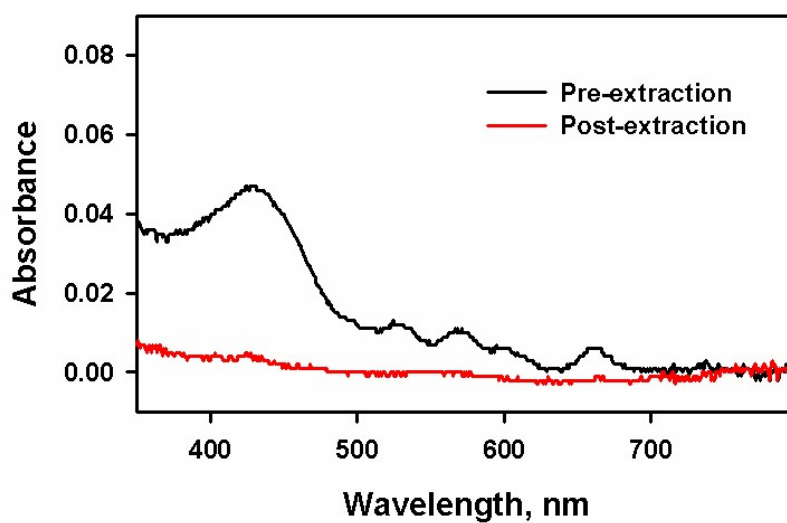


Fig. S15. UV-Visible spectra of compound **1** in aqueous phase before (black) and after (red) extraction with the water-saturated 1-octanol.

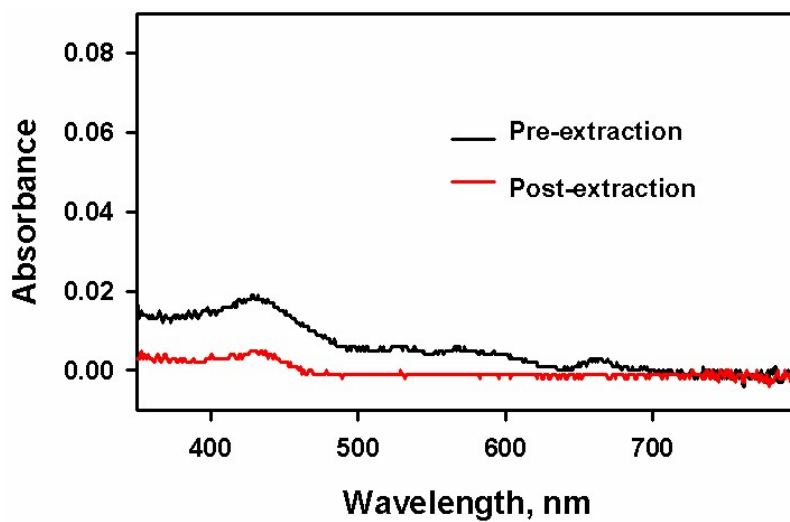


Fig. S16. UV-Visible spectra of compound **2** in aqueous phase before (black) and after (red) extraction with the water-saturated 1-octanol.

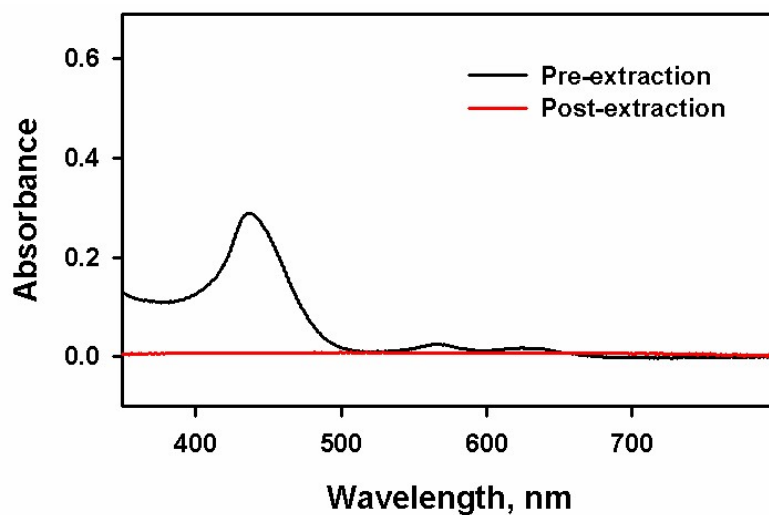


Fig. S17. UV-Visible spectra of compound **3** in aqueous phase before (black) and after (red) extraction with the water-saturated 1-octanol.

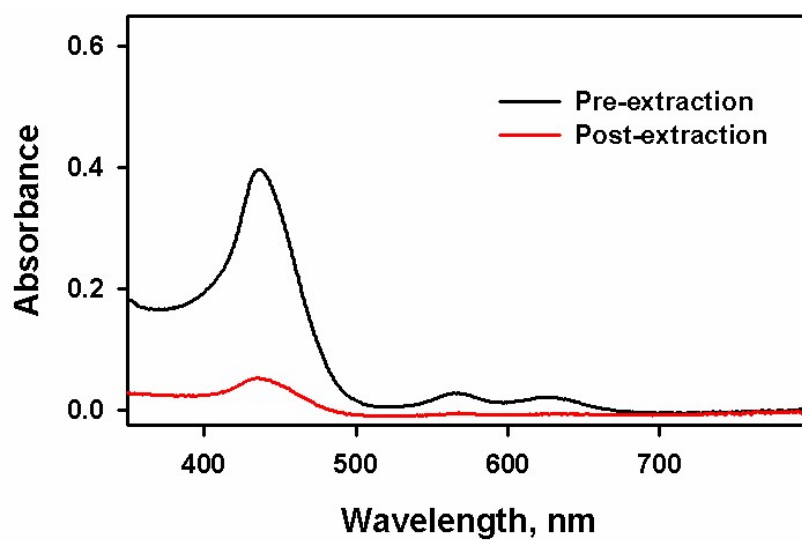


Fig. S18. UV-Visible spectra of compound **4** in aqueous phase before (black) and after (red) extraction with the water-saturated 1-octanol.

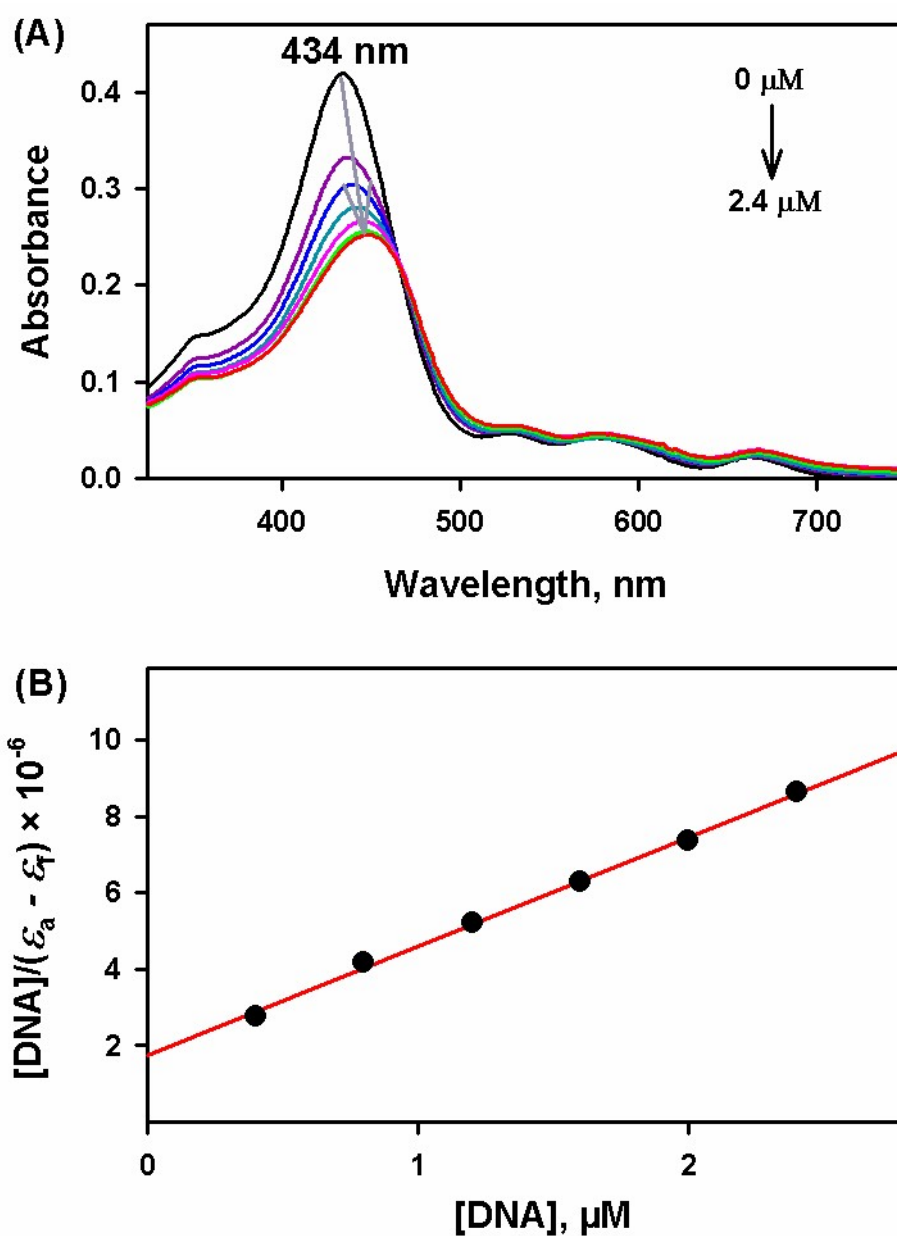


Fig. S19. (A) Absorption spectra of **2** in pH=7.2 buffer at 25 °C in the presence of the increasing amount of CT-DNA. $[\mathbf{2}] = 6 \mu\text{M}$, $[\text{DNA}] = \text{Increment of } 0.4 \mu\text{M}$. The grey arrow indicates the change in absorption upon increasing the DNA concentration. (B) A plot of $[\text{DNA}]/(\Delta\epsilon)$ vs. $[\text{DNA}]$.

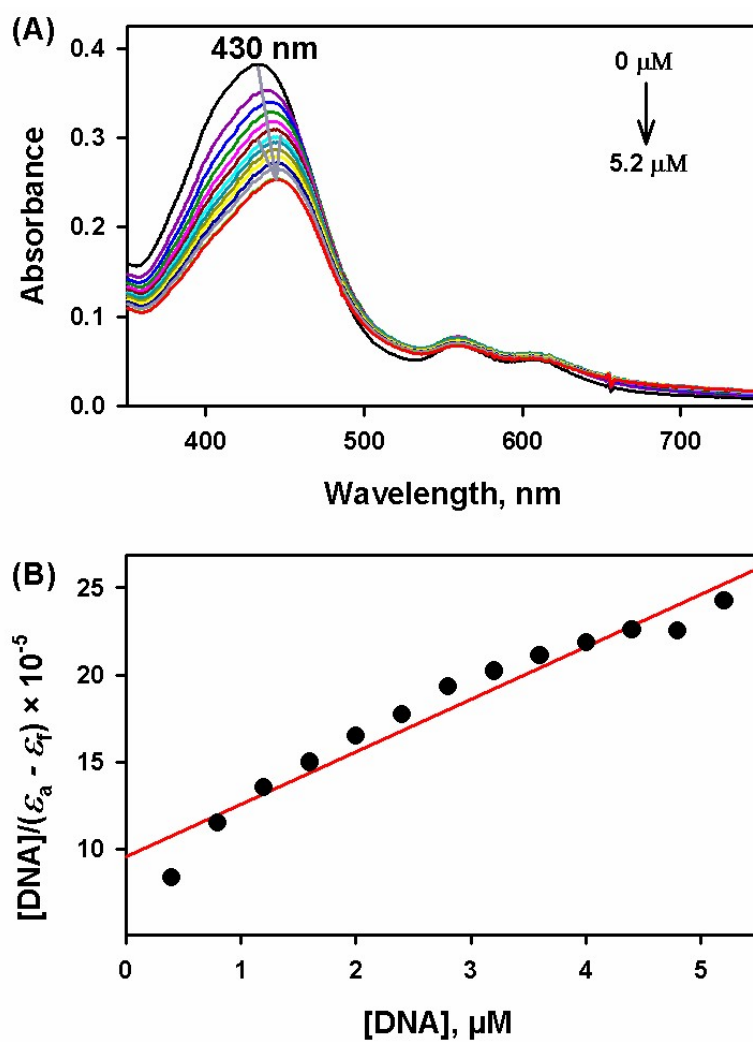


Fig. S20. (A) Absorption spectra of **3** in pH = 7.2 buffer at 25 °C in the presence of an increasing amount of CT-DNA. [**3**] = 6 μM, [DNA] = Increment of 0.4 μM. The grey arrow indicates the change in absorption upon increasing the DNA concentration. (B) A plot of $[DNA]/(\Delta\epsilon)$ vs. [DNA].

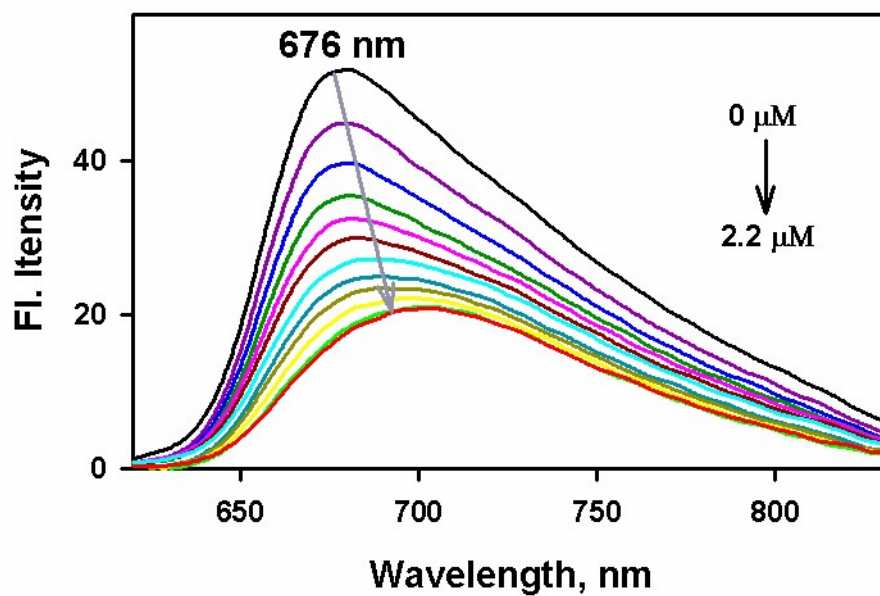


Fig. S21. Fluorescence emission spectra of **2** in pH = 7.2 buffer solution, with increasing concentration of CT-DNA. $[2] = 6 \mu\text{M}$, $[\text{DNA}] = \text{increment of } 0.2 \mu\text{M}$. The grey arrow indicates the change in emission intensity upon increasing the complex concentration.

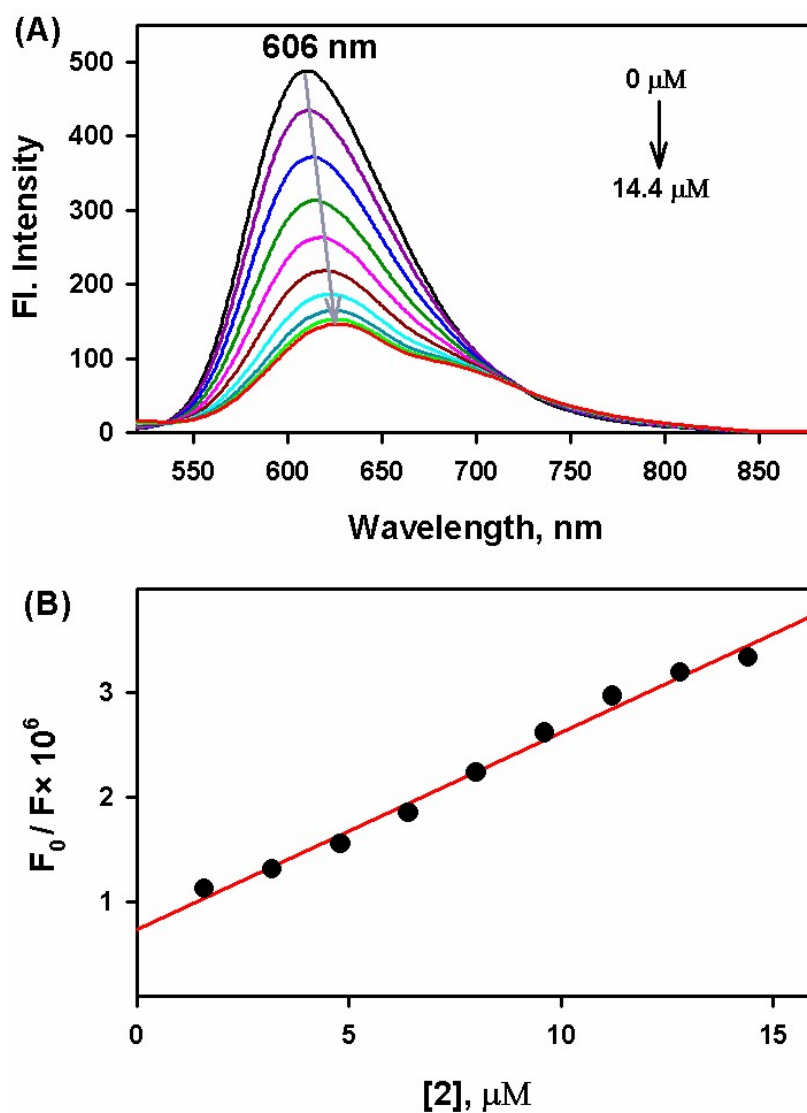


Fig. S22. (A) Emission spectra of EB bound to DNA in the presence of porphyrins, (A) 2 with increasing concentration of CT DNA. [DNA] = 12 μM , [EB] = 5 μM , [2] = 1.6 μM increment. The grey arrow indicates the change in emission intensity upon increasing the concentration of [2]. (B) Fluorescence quenching curve of EB bound DNA by the porphyrins.

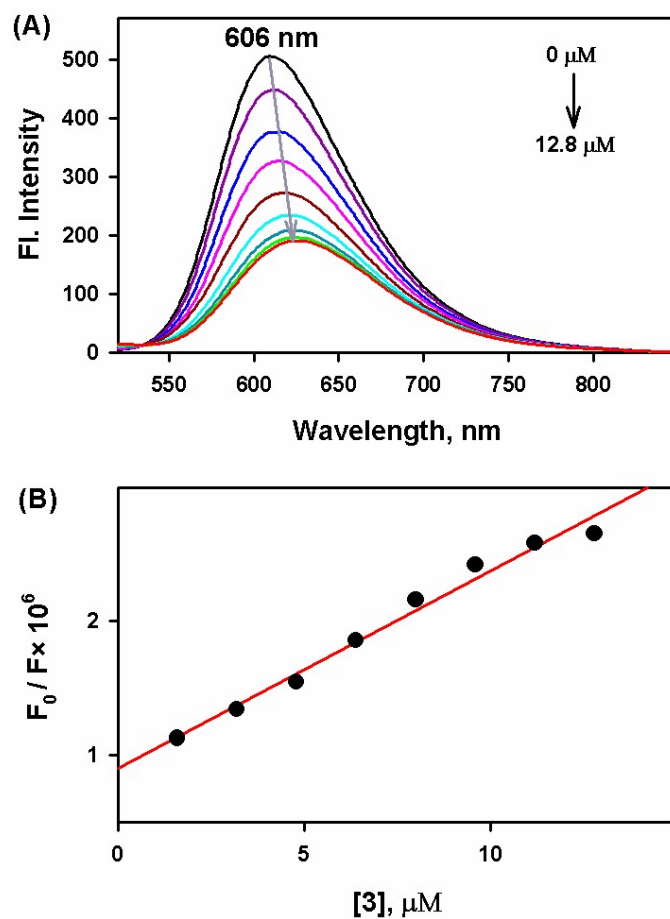


Fig. S23. Emission spectra of EB bound to DNA in the presence of porphyrins, (A) **3** with increasing concentration of CT DNA. [DNA] = 12 μM , [EB] = 5 μM , [**3**] = 1.6 μM increment. The grey arrow indicates the change in emission intensity upon increasing the concentration of [**3**] (B) Fluorescence quenching curve of EB bound DNA by the porphyrins.

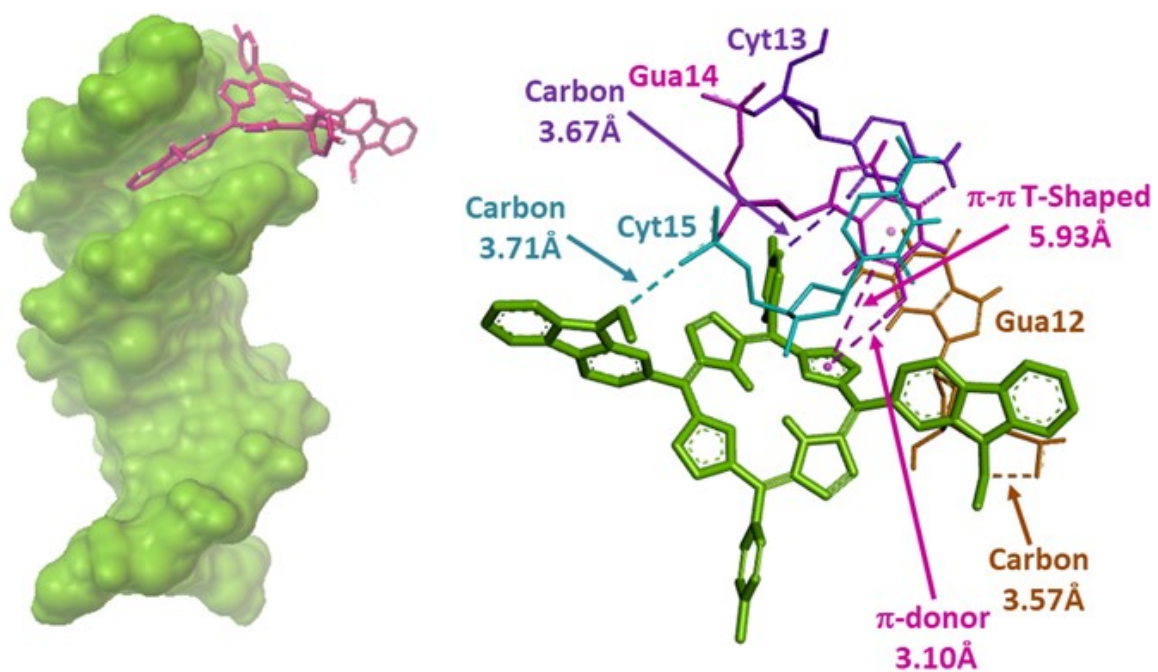


Fig. S24. Molecular docked structure and interactions of **2** with DNA.

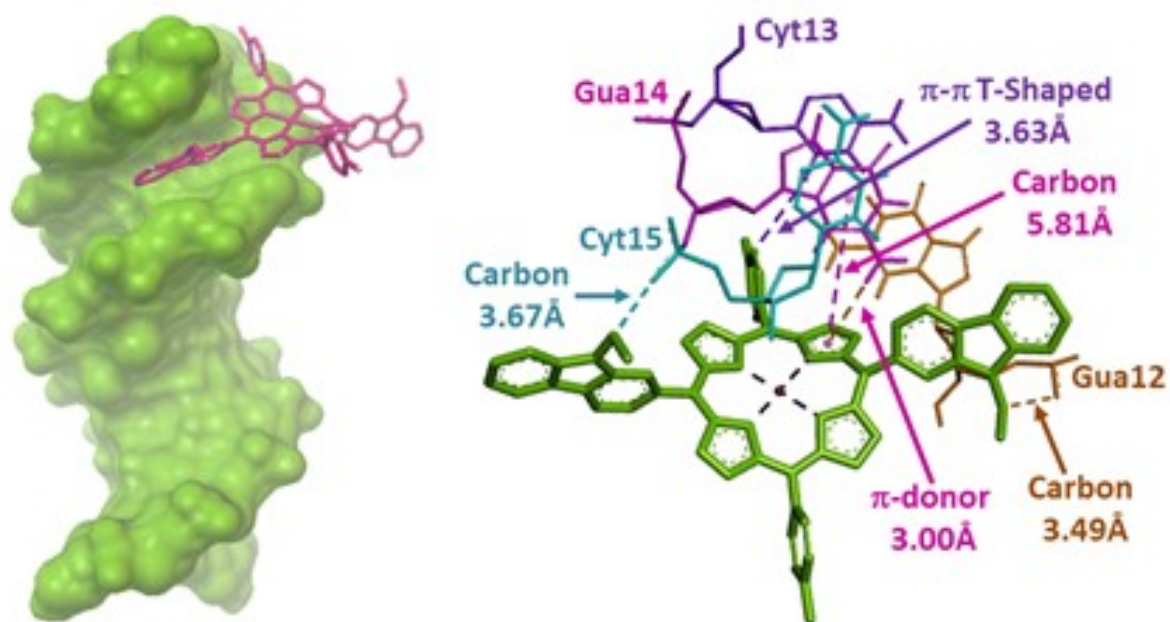


Fig. S25. Molecular docked structure and interactions of **3** with DNA.

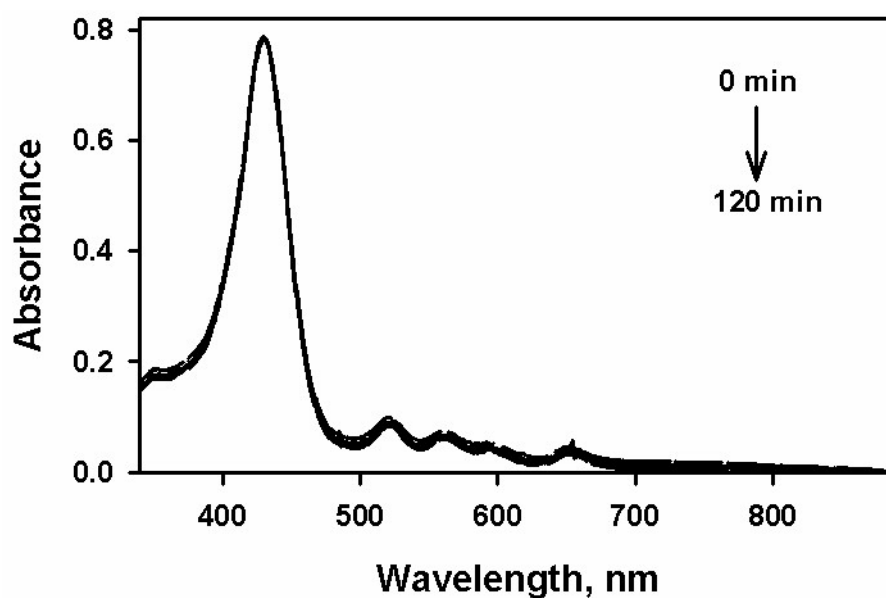


Fig. S26. The time-dependent absorption spectrum of compound **2** under the light source of $\lambda = 450\text{--}750\text{ nm}$, 15 J cm^{-2} .

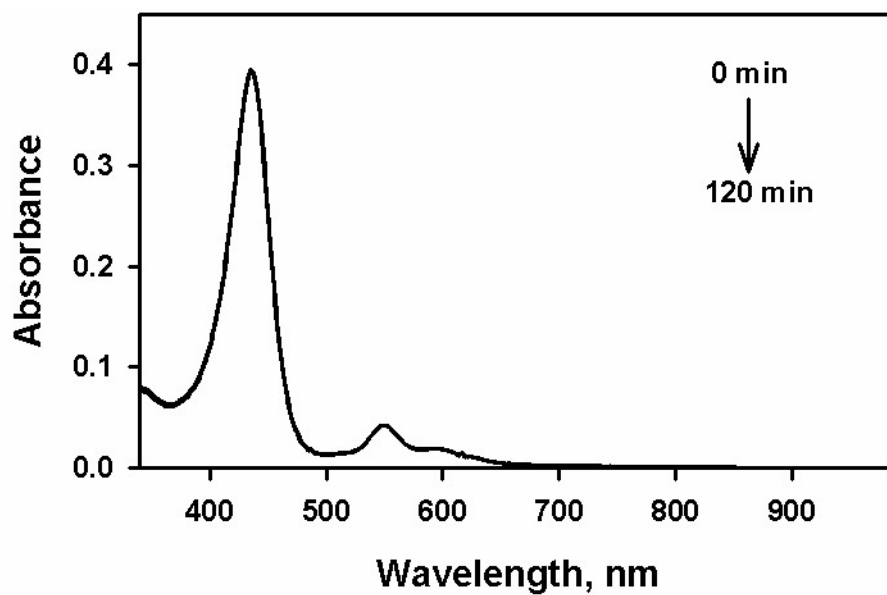


Fig. S27. The time-dependent absorption spectrum of compound **3** under the light source of $\lambda = 450\text{--}750\text{ nm}$, 15 J cm^{-2} .

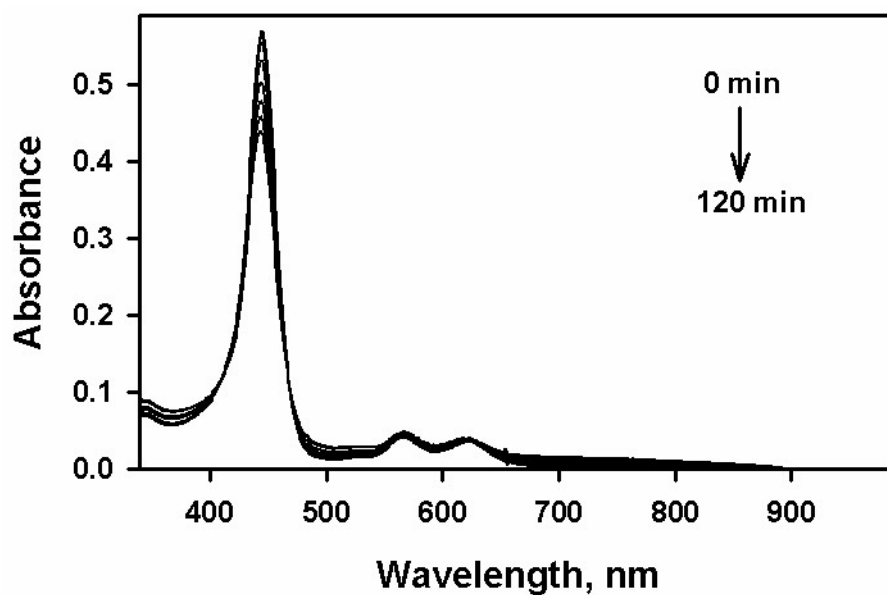


Fig. S28. The time-dependent absorption spectrum of compound **4** under the light source of $\lambda = 450\text{--}750\text{ nm}$, 15 J cm^{-2} .

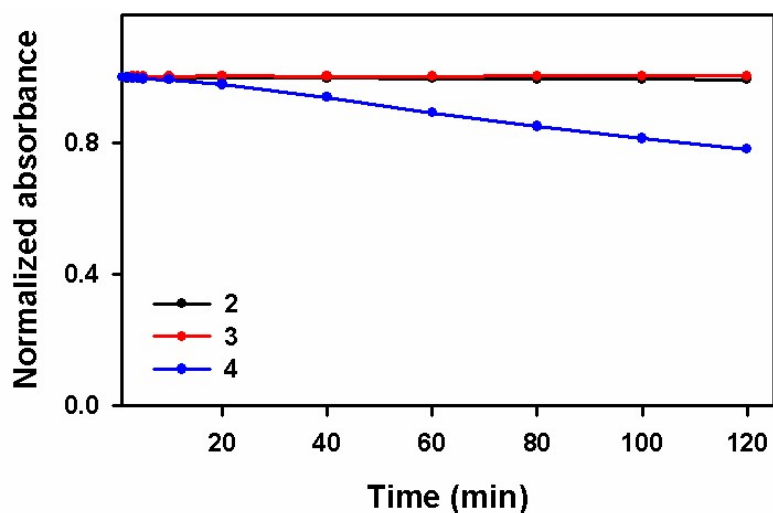


Fig. S29. Change in absorbance of compound 2-4 with an increase in time of irradiation under the light source of $\lambda = 450\text{--}750$ nm, 15 J cm^{-2} .

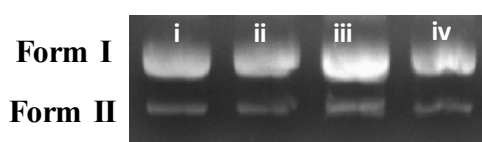


Fig. S30. Effect of NaN_3 on the cleavage in presence of compounds 2-4. Lane (i): DNA alone; Lane (ii): DNA+10 μM 2+ 50 μM NaN_3 ; Lane (iii): DNA+10 μM 3 + 50 μM NaN_3 ; Lane (iv): DNA+10 μM 4 + 50 μM NaN_3 .

Table S1 Electrochemical data of 2-4 in DMF using 0.1 M TBAHFP at 25°C .

Compound	$E_{1/2}(\text{oxd})/\text{V}$		$E_{1/2}(\text{red})/\text{V}$		Energy Level (eV)		ΔE (eV) (From CV)
					HOMO ^a	LUMO ^a	
H₂TPP¹	1.08	-	-1.11	-1.53	-5.48	-3.29	2.19
CuTPP¹	1.01	1.26	-1.19	-1.71	-5.41	-3.21	2.20
ZnTPP¹	0.79	1.38	-1.34	-1.73	-5.19	-3.06	2.13
2	0.69	1.04	-1.00	-1.71	-5.09	-3.40	1.69
3	0.68	1.01	-1.09	-1.80	-5.08	-3.31	1.77
4	0.54	0.99	-1.14	-1.66	-4.94	-3.26	1.68

^a $E_{\text{HOMO}} = -(E_{\text{oxd}} + 4.4) \text{ eV}$; $E_{\text{LUMO}} = -(E_{\text{red}} + 4.4) \text{ eV}$, ^a*Chem. Commun*, 48 (2012), 8377

¹ J. Ramesh, S. Sujatha and C. Arunkumar, *RSC Adv.*, 2016, **6**, 63271-63285.